Supplementary material

Anti-corrosion MgO nanoparticle equipped graphene oxide nanosheet for efficient room-temperature H_2S removal

Hai Xu,[a] *Yankai Pan,*[a] *Feng Hu,*[a] *Bo Niu,*[a] *Yayun Zhang,*[a,b,*] *and Donghui Long,*[a,b,*]

[a] State Key Laboratory of Chemical Engineering, East China University of Science and Technology, Shanghai 200237, China.

[b] Shanghai Key Laboratory of Multiphase Materials Chemical Engineering, East China University of Science and Technology, Shanghai 200237, China.

* Corresponding authors: longdh@mail.ecust.edu.cn (Donghui Long),

yy.zhang@ecust.edu.cn (Yayun Zhang)

ABSTRACT: Metal oxides has emerged promising potential in catalytic oxidation of H_2S at room temperature, but is currently challenged by a low catalytic performance and tendency to be corroded in acid reaction surroundings. Herein, we report a facile strategy to prepare a series of ultrafine metal oxide nanoparticles loaded on reduced graphene oxide (rGO) for efficient H_2S catalytic oxidation at room temperature. The hyper-dispersed nanoparticles solve the stacking of rGO to maintain the two-dimensional sheet structure, breaking through the limits of traditional porous carbons with easy blockage of nanopores and low porosity, thereby offering large sulfur storage depot. Meanwhile, higher density of alkaline sites is provided for catalytic reaction and synergistically enhances the desulfurization performance. Further, Density functional theory (DFT) calculation is employed for interpreting involved mechanism and find that MgO crystal, with larger band gap and poorer degree of its bands mixing with H_2S orbitals, possesses lower reactivity towards H_2S corresponding to the strong corrosion resistance. Hence, MgO/rGO composite exhibits an excellent catalytic activity with breakthrough capacity of 3110 mg/g, higher than the other counterparts. The current work could contribute new insights into synergistic catalytic oxidation mechanism of H_2S by metal oxides and carbon-based composites, which provides theoretical basis for the design and development of efficient room-temperature desulfurizers.

Keywords: Metal oxides, Ultrafine nanoparticles, Graphene oxide, Room-temperature H_2S oxidation, Catalytic mechanism

1. Supplementary Figures

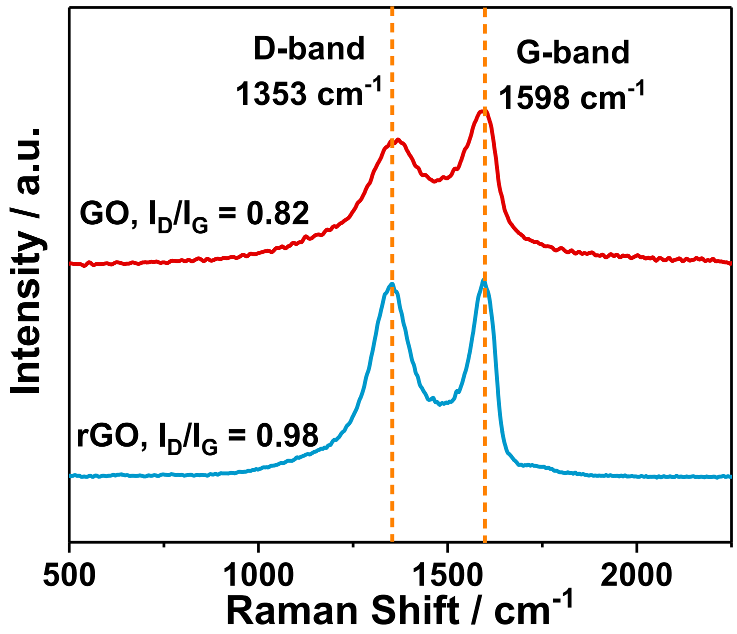

Figure S1. Raman spectra of the GO and rGO.

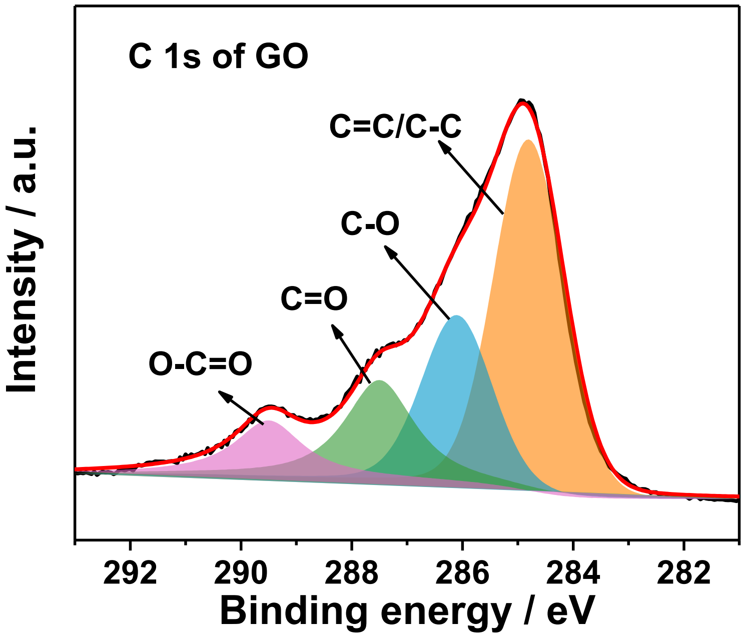

Figure S2. High-resolution C 1s spectra of the GO.

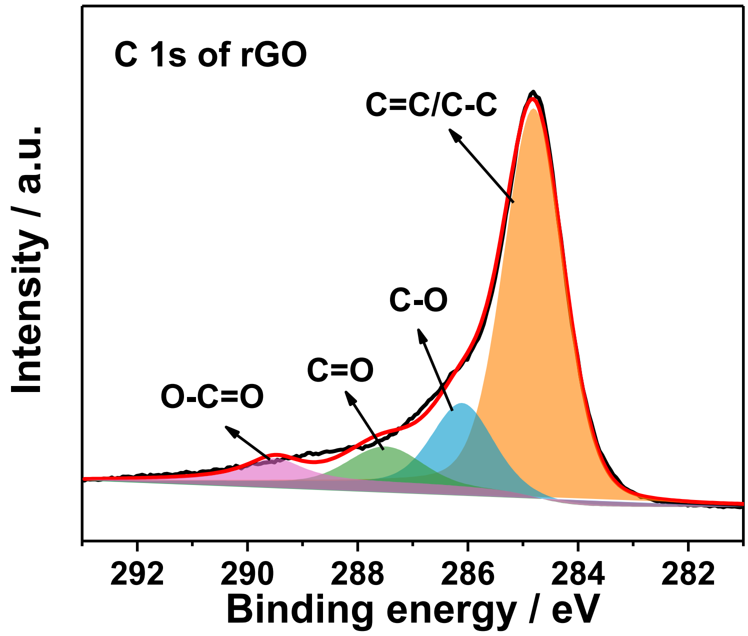

Figure S3. High-resolution C 1s spectra of the rGO.

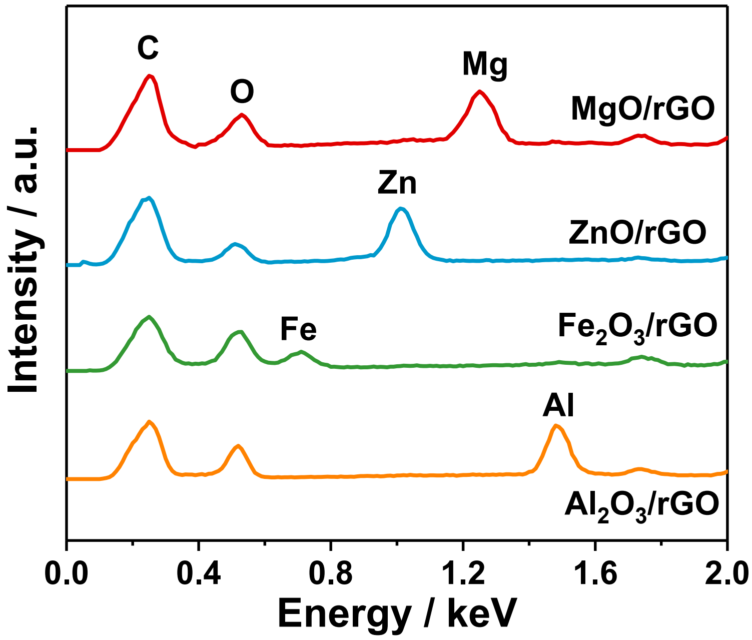

Figure S4. EDX spectra and of the metal oxide/rGO.

It can be found from the EDX spectrum that the metal oxide/rGO composite is mainly composed of C, O and corresponding metal elements, and there are no other impurity elements.

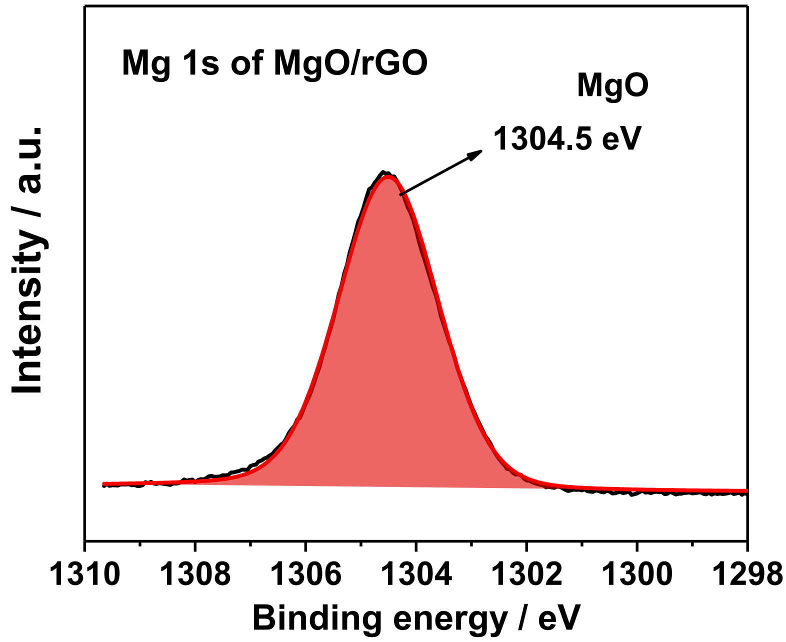

Figure S5. High-resolution Zn 2p spectrum of MgO/rGO.

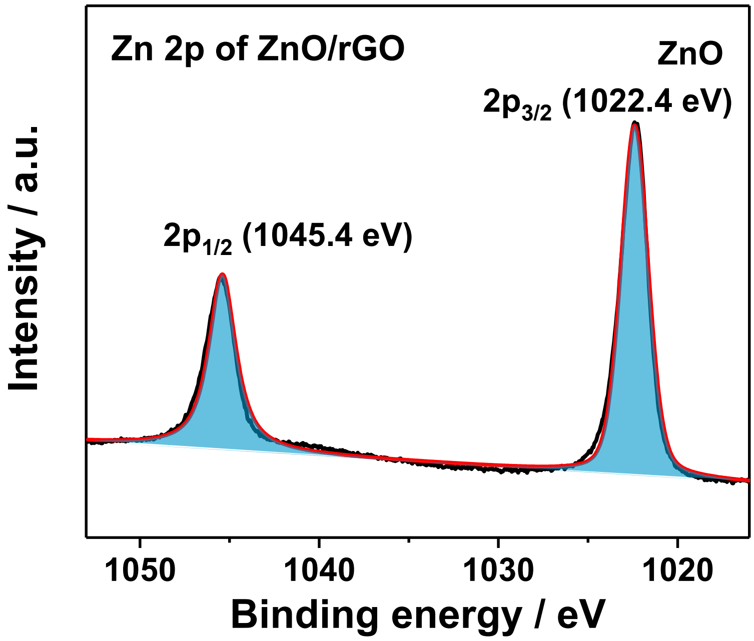

Figure S6. High-resolution Zn 2p spectrum of ZnO/rGO.

For the high-resolution Zn 2p spectrum of Zn /rGO, it can be divided into two peaks at 1022.4 eV and 1045.4 eV, corresponding to $2p_{3/2}$ and $2p_{1/2}$ splitting peaks in ZnO[1].

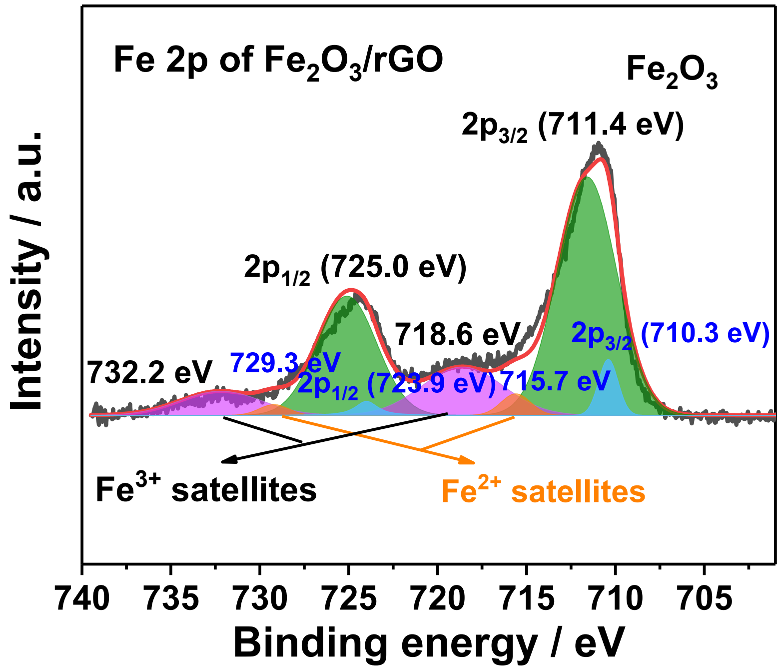

Figure S7. High-resolution Fe 2p spectrum of Fe_2O_3/rGO.

The high-resolution Fe 2p spectrum of Fe_2O_3/rGO can be divided into eight peaks, of which the sub peaks at 711.4 eV and 725.0 eV belong to $2p_{3/2}$ and $2p_{1/2}$ splitting peaks in Fe_2O_3, and the sub peaks at 718.6 eV and 732.2 eV belong to Fe^{3+} satellite peaks[2], and the sub peaks at 710.3 eV and 723.9 eV belong to $2p_{3/2}$ and $2p_{1/2}$ splitting peaks in FeO, and the sub peaks at 715.7 eV and 729.3 eV belong to Fe^{2+} satellite peaks.

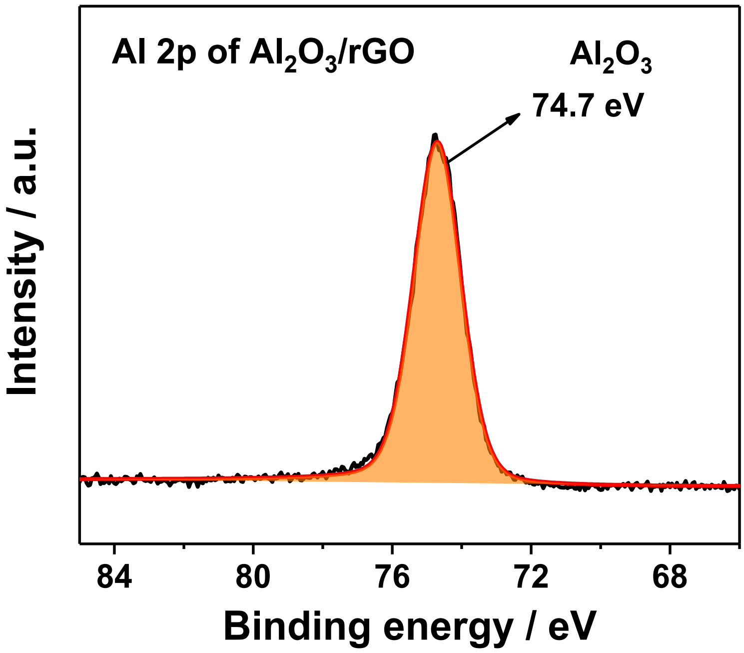

Figure S8. High-resolution Al 2p spectrum of Al_2O_3/rGO

The high-resolution Al 2p spectrum of Al_2O_3/rGO shows that there is only a single peak at 74.7 eV, corresponding to the bonding of Al_2O_3[3].

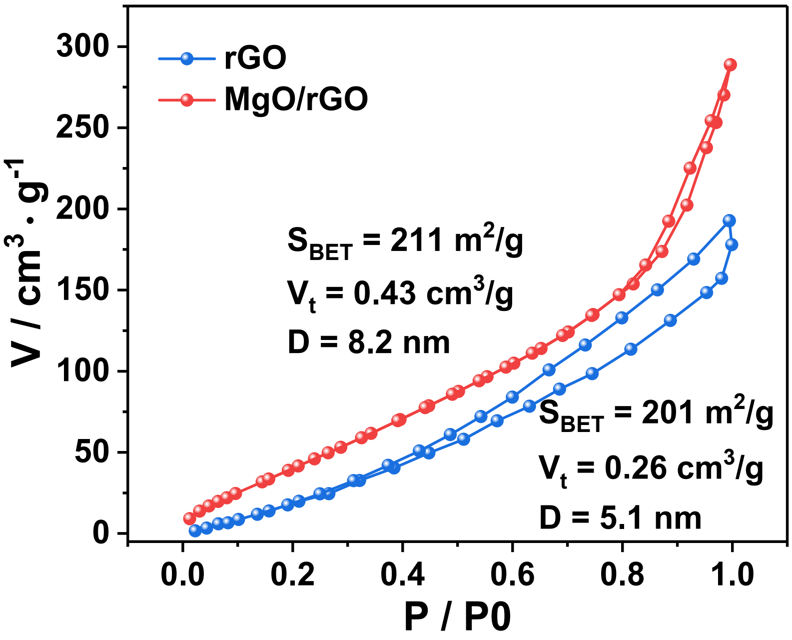

Figure S9. N_2 adsorption-desorption isotherms of rGO and MgO/rGO.

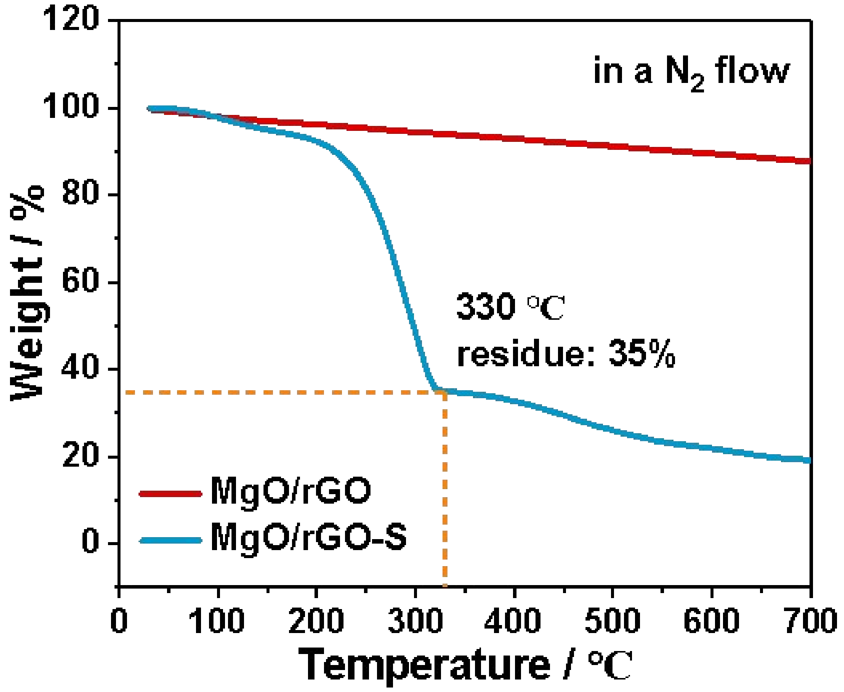

Figure S10. TG curves of the MgO/rGO catalyst before and after desulfurization.

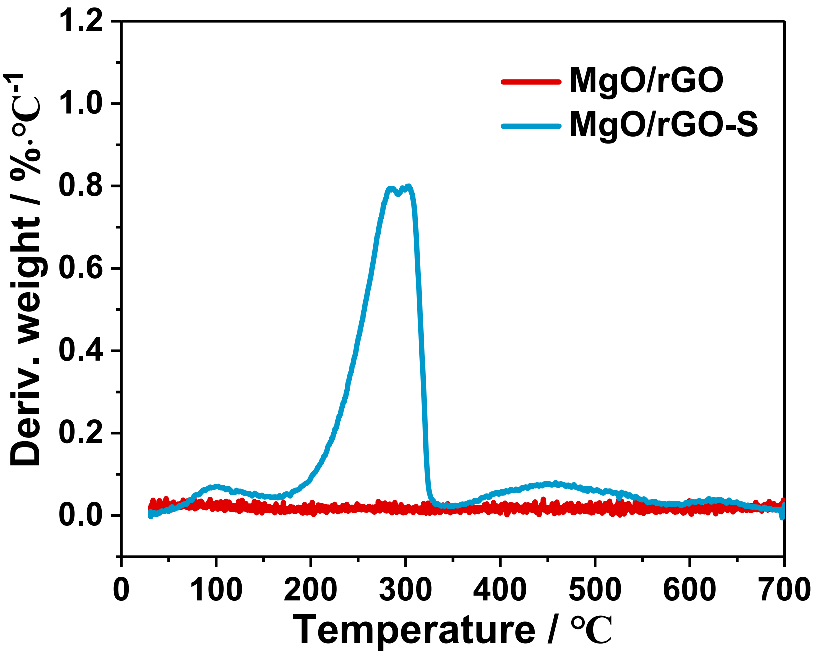

Figure S11. DTG curves of the MgO/rGO catalyst before and after desulfurization.

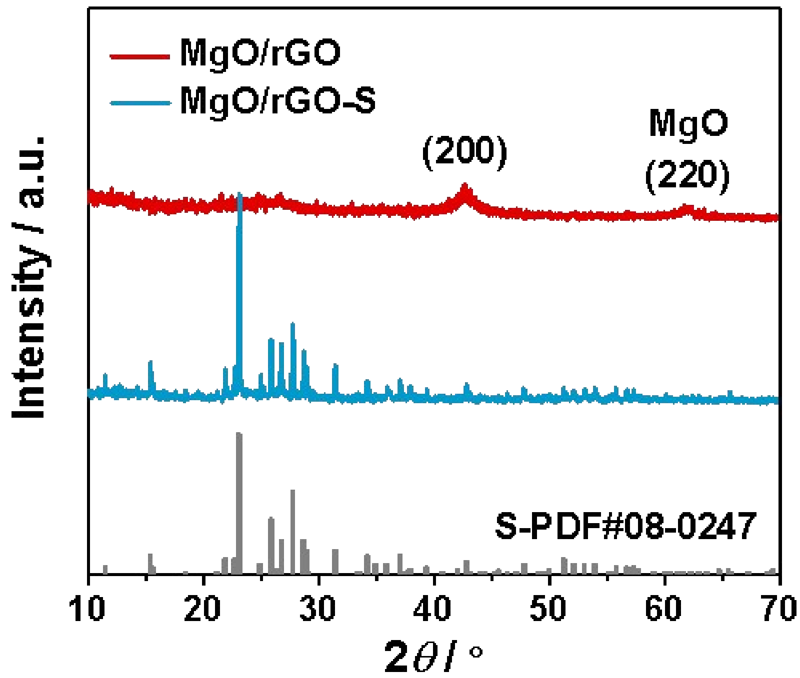

Figure S12. XRD patterns of the MgO/rGO catalyst before and after desulfurization.

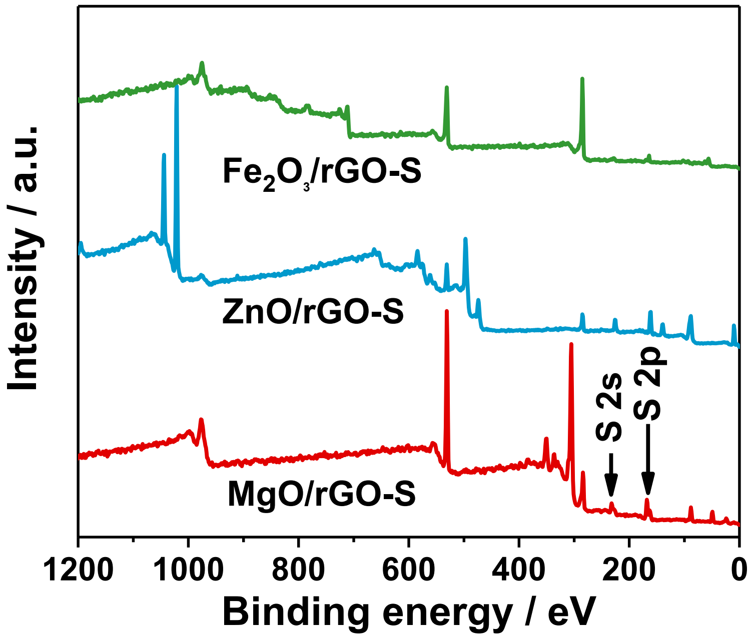

Figure S13. XPS spectra of the metal oxide/rGO-S.

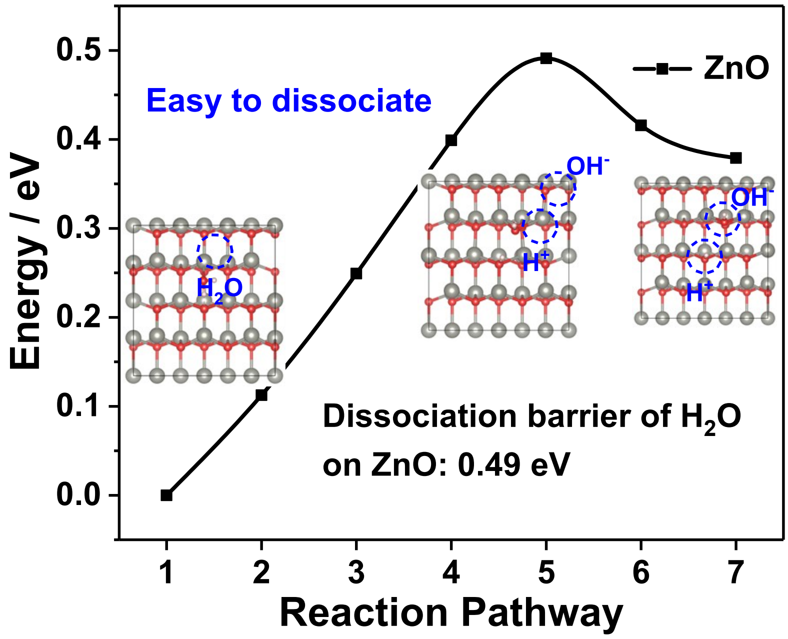

Figure S14. The reaction energy and path for $H_2O \rightarrow H + OH$ on the surface of ZnO crystal (100).

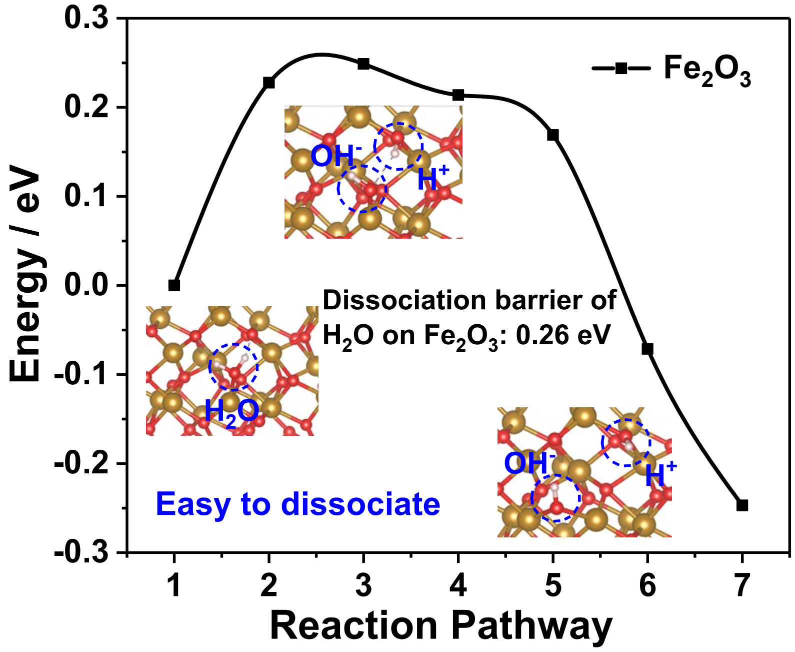

Figure S15. The reaction energy and path for $H_2O \rightarrow H + OH$ on the surface of Fe_2O_3 crystal (311).

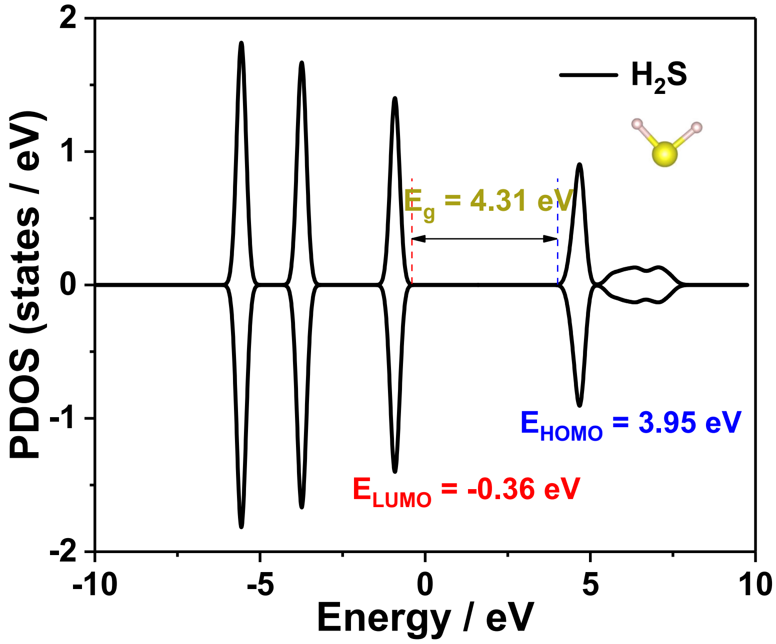

Figure S16. Partial density of states (PDOS) of H_2S in gas phase.

2. Supplementary Tables

Table S1. Functional group contents of GO and rGO resulted from C 1s spectra

samples	C=C/C-C	C-O	C=O	O-C=O
GO	49.6%	25.5%	13.1%	11.8 %
rGO	71.2%	15.7%	7.5%	5.6%

Table S2. Elemental analysis of GO and rGO

samples	C (wt.%)	H(wt.%)	O (wt.%)
GO	51.94	3.1	45.05
rGO	77.74	1.57	20.69

Table S3. The deconvolutionized peak positions and the corresponding ferrum species from Fe 2p analysis.

samples	composition of Fe speciesm	
	Fe_2O_3 (Fe^{3+}): 711.4 eV (Fe $2p_{3/2}$), 725.0 eV (Fe $2p_{1/2}$)	FeO (Fe^{2+}): 710.3 eV (Fe $2p_{3/2}$), 723.9 eV (Fe $2p_{1/2}$)
Fe_2O_3/rGO	91.6%	8.4%

Table S4. The acid-basic property of the composites, including rGO, MgO/ rGO and Fe_2O_3/rGO.

samples	rGO	MgO/ rGO	Fe_2O_3/rGO
PH	5.8	11.1	7.1

Table S5. The deconvolutionized peak positions and the corresponding sulfur species from S 2p analysis.

samples	composition of S speciesm		
	sulfide (S^{-2}): 161.4 eV (S $2p_{3/2}$), 162.6 eV (S $2p_{1/2}$)	sulfur (S^0): 164.0 eV (S $2p_{3/2}$), 165.2 eV (S $2p_{1/2}$)	sulfate (S^{+6}): 168.8 eV (S $2p_{3/2}$), 170.0 eV (S $2p_{1/2}$)
MgO/rGO-S	0%	89.0%	11.0%
ZnO/rGO-S	77.7%	14.0%	8.3%
Fe2O3/rGO-S	80.7%	11.0%	8.3%

ASSOCIATED CONTENT

Supporting Information

AUTHOR INFORMATION

Corresponding Authors

* E-mail: longdh@mail.ecust.edu.cn (Donghui Long)

* E-mail: yy.zhang@ecust.edu.cn (Yayun Zhang)

ORCID

Donghui Long: http://orcid.org/0000-0002-3179-4822

Yayun Zhang: http://orcid.org/0000-0002-1714-3126

Yankai Pan: http://orcid.org/0000-0003-2604-7942

Notes

The authors declare no competing financial interest.

ACKNOWLEDGMENT

This work was financially supported by National Natural Science Foundation of China (No. 22008073, No. 21878091, No. 22078100, No. 52102098), Shanghai Sailing Program (No. 20YF1410600), Fundamental Research Funds for the Central Universities (222201718002), and Shanghai Talent Development Fund (2021026).

REFERENCES

[1] Saáedi, A.; Yousefi, R.; Jamali-Sheini, F.; Zak, A. K.; Cheraghizade, M.; Mahmoudian, M.; Baghchesara, M. A.; Dezaki, A. S., XPS studies and photocurrent applications of alkali-metals-doped ZnO nanoparticles under visible illumination conditions. *Physica E: Low-dimensional Systems and Nanostructures* **2016,** *79*, 113-118.

[2] Flak, D.; Chen, Q.; Mun, B. S.; Liu, Z.; Rękas, M.; Braun, A., In situ ambient pressure XPS observation of surface chemistry and electronic structure of α-Fe_2O_3 and γ-Fe_2O_3 nanoparticles. *Applied Surface Science* **2018,** *455*, 1019-1028.
[3] Kim, D. S.; Kim, Y. E.; Kim, H., Improved fast charging capability of graphite anodes via amorphous Al_2O_3 coating for high power lithium ion batteries. *Journal of Power Sources* **2019,** *422*, 18-24.